ELSEVIER

Nuclear Instruments and Methods in Physics Research B 193 (2002) 762–767

NIM B
Beam Interactions with Materials & Atoms

www.elsevier.com/locate/nimb

Dynamics of secondary ion emission: Novel energy and angular spectrometry

T. Jalowy [a,*], R. Neugebauer [a], M. Hattass [a], J. Fiol [a,1], F. Afaneh [a,2], J.A.M. Pereira [b], V. Collado [b], E.F. da Silveira [b], H. Schmidt-Böcking [a], K.O. Groeneveld [a]

[a] *Institut für Kernphysik der J.W. Goethe Universität, August-Euler-Str. 6, D-60486 Frankfurt am Main, Germany*
[b] *Depto. de Física, Pontifícia Universidade Católica, CP 38071, 22952-970 Rio de Janeiro, Brazil*

Abstract

A new spectrometer has been developed based on the combination of standard time-of-flight technique and position sensitive delay line detectors. The basic features of the spectrometer, particularly of the multi-hit capable detector, are described. To demonstrate the performance of this new system, the dynamic emission characteristics, i.e. the three-dimensional velocity distribution, of desorbed H_2^+ from Al target by Ar^0 impact (570 keV) is presented. It is found that the desorption yield is maximum for radial and axial emission velocities at 1.2 and 12 km/s respectively, corresponding to 1.5 eV ions emitted at 57° to normal (following the projectile radial direction). The initial energy distribution spreads out over 16 eV.

PACS: 34.50.Dy; 39.90.+d
Keywords: Ion solid interaction; Secondary ion mass spectrometry; Time-of-flight-technique and position sensitive detectors; Energy and angle differential spectrometry; Secondary ion desorption

1. Introduction

An energetic projectile traversing a solid transfers continuously its kinetic energy by interacting with the atoms and electrons. The energy deposition leads to track formation inside the solid and to emission of secondary particles as secondary atoms, molecules or clusters (charged or neutral) and electrons. There are several mechanisms which contribute to the emission process and the track creation. Therefore, the emitted particles can be used as messengers for the track formation, enlightening the basic interactions inside the solid. We focus on the emission of positive secondary ions emitted from the projectile entrance surface.

The analysis on the secondary ion emission yields from solids under fast ion impact have been published frequently in the past, e.g. [1–6]. However, there are relatively few data on the dynamic

* Corresponding author. Tel.: +49-69-798-24291/24238; fax: +49-69-798-24212.
E-mail address: jalowy@hsb.uni-frankfurt.de (T. Jalowy).
[1] Permanent address: Céntro Atómico Bariloche and Instituto Balseiro, CNEA, Bariloche, Argentina.
[2] Permanent address: Department of Physics, Hashemit University, Zarqa 13115, Jordan.

0168-583X/02/$ - see front matter
PII: S0168-583X(02)00900-X

emission characteristics, i.e. mass separated vector velocity distribution of secondary ion, e.g. [7–9]. The study of the dynamics provides direct access to the basic interaction mechanism of projectile ions with solid surfaces.

For the measurement of the dynamic emission characteristics of emitted secondary ions from ion–solid-collisions a new spectrometer has been developed. This spectrometer is based on the (used successfully in gas target experiments) COLTRIMS-system (cold target recoil ions momentum spectroscopy) developed by Schmidt-Böcking and collaborators in Frankfurt a.M. [10–12]. This system has been further developed and applied to energy and angle differential spectrometry of secondary ions emitted in ion–solid-collisions.

2. Spectrometer

The principles and the sketch of the spectrometer are shown in Figs. 1 and 2. The charged particles produced in the impact (secondary electrons or secondary ions) are directed to two-dimensional multi-hit detectors (Fig. 1) by an uniform field perpendicular to the target surface. The position and the time-of-flight (TOF) signals yield the three components of the initial momentum, i.e. the total energy and the emission angles of the secondary ions. By choosing the corresponding polarity of the extraction voltage it is possible to order all emitted charged particles according to their TOF and detect them sequentially. Moreover, the multi-hit capability of the position sensitive detector provides the possibility to acquire simultaneously charged particles even with the same mass, produced in the collision. The complex data acquisition and analysis is realized by the powerful PC-based system CoboldPC [13].

In contrast to ordinary TOF spectrometry, using the combination of one high extraction field with a drift tube to increase mass resolution, we have used only one extraction region (8.3 cm long). The reason of having used an extended extraction region is to obtain a better axial energy resolution by getting a broader TOF-peak. In this single region spectrometer, two different extraction potentials (3 kV and 600 V) have been employed: the higher extraction voltage allows detection of secondary ions with large radial energies ($\geqslant 50$ eV), while the lower extraction voltage improves the energy resolution of low radial energy ions.

The homogeneous electric field perpendicular to the target and the detector is maintained by a sequence of equidistant electrodes connected with identical resistors. The projectile beam enters the spectrometer through slits in the electrodes, traverses a thin target and is detected by a multichannelplate (MCP) detector. The dimensions of the slits inside the electrodes are designed in such a way, that a microbeam can easily enter in the spectrometer without having field disturbance in the sensitive central part of the spectrometer. The target is fixed on a holder connected to an external manipulator. The whole spectrometer is placed on a rotation device, which allows incidence projectile angles from 36° up to 80° with respect to the normal. This design enables to study simultaneously the emission of secondary particles both from the projectile entrance and exit side if two position sensitive detectors are employed.

The following coordinate system has been defined in the experiment: z is the axis normal to the target plane, x and z axes define the incidence plane of the beam; y-axis is perpendicular to the incidence plane. Therefore, it is expected a reflection symmetry of the data in the y-direction.

3. TOF measurement

The calculation of both the axial and the radial velocities requires a knowledge of the absolute TOF of each emitted particle. A precise start signal for the TOF measurement is provided by secondary electrons emitted and extracted from the rear target surface to a MCP detector. By using a extraction field of 2 kV/cm, their initial energy distribution plays a minor role in the TOF spectrum resolution. As a quality control for this method, the width of the photon peak could be used as reference: its FWHM is about 1.5 ns (Fig. 3(a)). The spectrometer can be rotated by 180° for analysis of the secondary ion emission from the rear target surface.

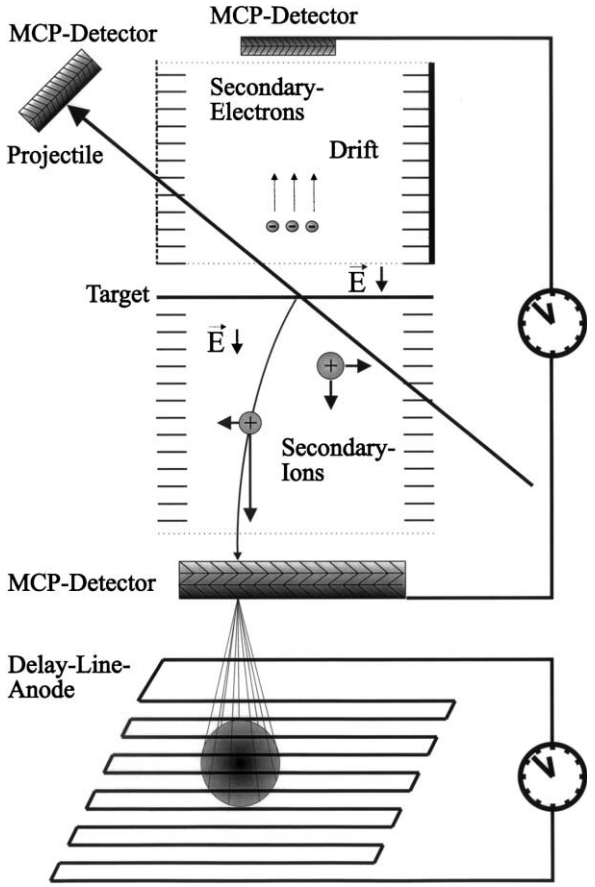

Fig. 1. Schematic signal production and signal paths illustrate the determination of position and TOF.

4. Position measurement

The x–y-position measurement is provided by a MCP detector equipped with a delay line anode for position sensitive readout [14,15]. The secondary ion impinging on the MCP array induces locally a secondary electron avalanche. The produced charge cloud is collected on two parallel sets of spiralled wires. The signals induced on the wires propagate along the wires and an electronic clock measures the signals arriving at both ends (see Fig. 1). These time intervals of signals are proportional to the position of the charge cloud in each dimension. This delay method allows high counting rate (up to MHz) and the measurement of in multi-hit mode, i.e. more than one particle impinging on the detector per event can be registered and constitutes an important tool for correlation analysis among the emitted particles. This feature is a significant improvement compared to the charge dividing method used e.g. in the backgammon (wedge and strip) anode.

5. Experimental results and discussion

The experiments were performed at the 2.5 MV van de Graaff accelerator at the Institut für Kernphysik der J.W. Goethe Universität in Frankfurt am Main. We have selected for presentation the data corresponding to the emission of H_2^+ secondary ions (from the projectile entrance surface) from an Al target (2000 Å) bombarded by Ar^0 (570 keV, 3–5 $\times$ 10^3 projectiles/s), at incident angle

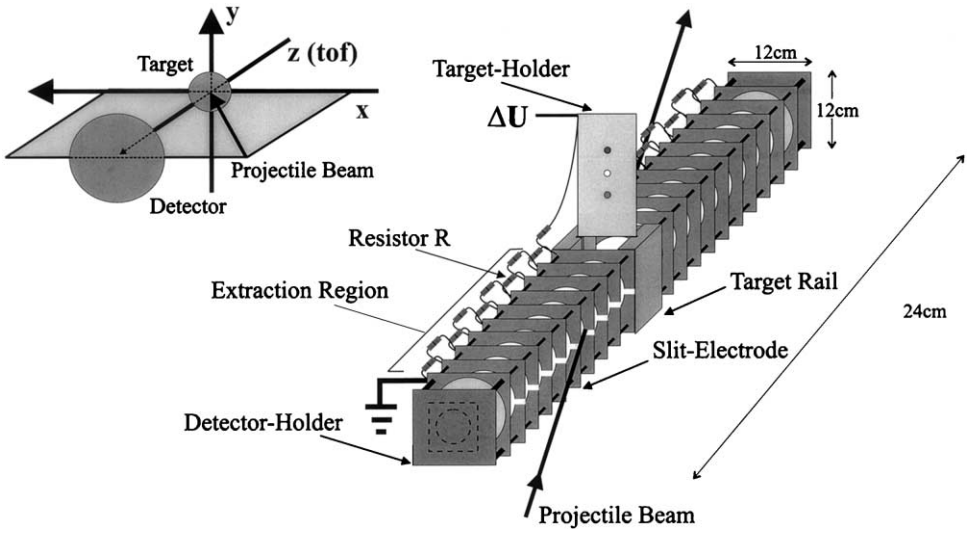

Fig. 2. Schematic experimental setup with coordinate labeling as insert.

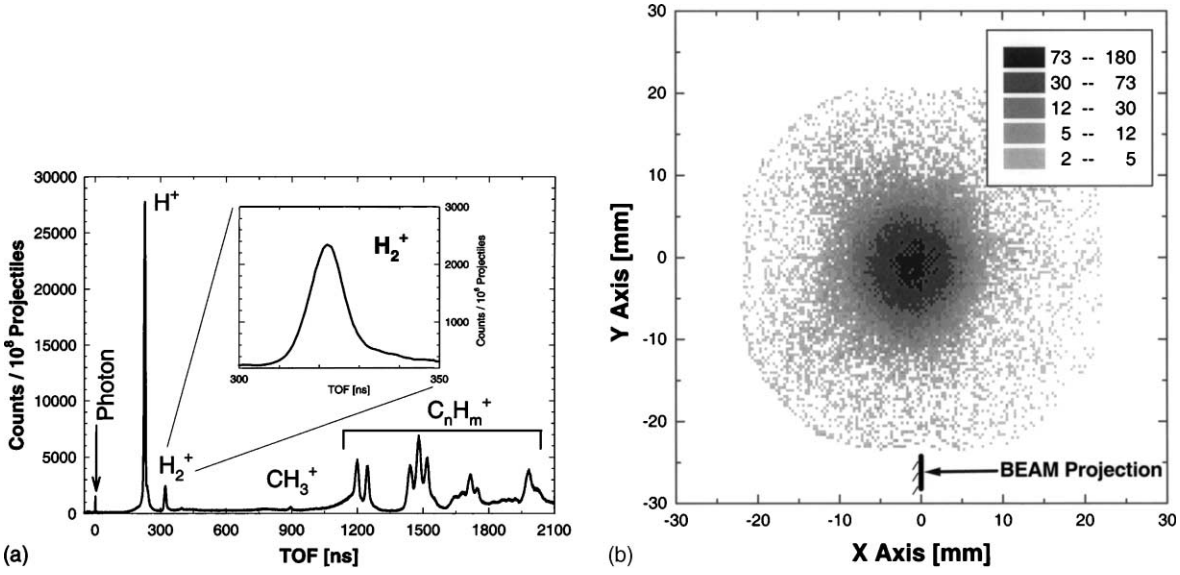

Fig. 3. (a) Secondary ion TOF-spectrum from Ar^0 (570 keV) → Al (2000 Å) collision obtained with 3 kV target extraction voltage. A zoom of mass 2 is inserted. (b) *x*–*y*-signal image of the detector with the intensity coded by grey values.

of 45° and under high vacuum conditions (5×10^{-7} hPa).

As H_2 is the most abundant constituent of residual gas at these pressures, it is always present at the sample surface accompanied by hydrocarbon molecules. Fig. 3(a) shows a typical TOF spectrum for surface masses up to $m = 70$ u corresponding to surface contaminants and their fragments. After the collision, the produced aluminium ions are neutralized traversing the adsorbed layers, so that they cannot be detected by this system.

H_2^+ was chosen to illustrate the treatment of the data by transforming the measured TOF and x–y-position in the detector into initial velocities distributions, i.e. velocity distribution in the source system. In Fig. 3(b) is presented the x–y-distribution for H_2^+. The three-dimension plot is constructed by the two dimensions (x and y) of the detector plane and by the measured emission yields represented by grey densities.

The TOF (given by the z-coordinate) provides the information about the axial velocity and the position (x–y-coordinates) about the radial velocity. To overcome this separation of axial and radial components the x–y-image was projected on both the x-axis and the y-axis and displayed as a function of TOF.

The transformation to velocities (km/s) is shown in Fig. 4(a) and (b), respectively for the y–z and x–y plots. Detailed information about the calibration and the transformation procedure is given in [16]. The v_y–v_z-distribution shows velocities in the 0–40 km/s range and is symmetric for positive and negative y, as expected. In contrast, the symmetry is broken in the x–z-plane because of the 45° incidence beam angle (see Fig. 3(b)). The same feature is also visible in the v_x–v_z-plot, as shown in Fig. 4. These results show that a fraction of the H_2^+ secondary ions is emitted by a process that still keep the memory of the direction of the projectile. The observed velocities correspond to initial energies in the 0–16 eV range, values which are smaller than those reported by the results of Most et al. [9], obtained for 1 MeV/u ^{127}I beam. The angle of maximum desorption yield is approximately 5.7° with respect to the target normal, corresponding to $v_x = -1.2$ km/s, $v_y = 0$ and $v_z = 12$ km/s. As the projectile velocity components are $v_{px} = v_{pz} = -1200$ km/s and $v_y = 0$, the nega-

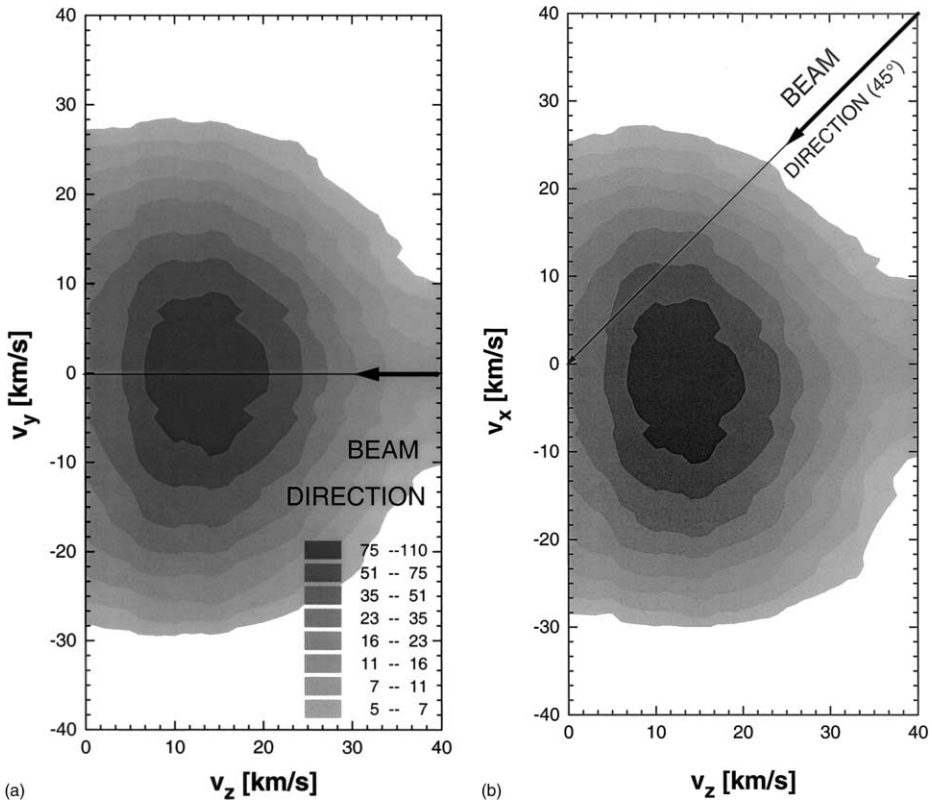

Fig. 4. (a) The v_y–v_z-spectrum (in km/s) of mass 2 (same experimental conditions as in Fig. 3). (b) The v_x–v_z-spectrum (in km/s) of mass 2.

tive velocity of the H_2^+ ions means that they are mostly desorbed in the same radial direction as the beam.

6. Conclusions

A TOF and position sensitive spectrometer was developed for initial energy and emission angle measurements of secondary ions. The obtained results show that this spectrometer is well suited for such studies.

Analysis of H_2^+ secondary ions illustrates the spectrometer capabilities. The TOF spectrum combined with the detected secondary ion x–y-distribution was transformed into v_x–v_y–v_z-velocity-distribution plots. It was found that the H_2^+ emission still remembers the projectile direction. Similar experiments with this x–y-TOF-spectrometer are under way.

Acknowledgements

We gratefully acknowledge DAAD-Bonn, BMBF at DLR-Bonn, VW-Stiftung, Willkomm-Stiftung-Frankfurt a.M. (Germany), CAPES/PROBRAL and FAPERJ (Brazil) for supporting this work.

References

[1] P. Sigmund, Lectures on Collision Theory, Report Fysik Insitut, Odense University, 1972.
[2] P. Häkansson, B. Sundqvist, Radiat. Eff. 61 (1982) 179.
[3] A. Albers, K. Wien, P. Dück, W. Treu, H. Voit, Nucl. Instr. and Meth. 198 (1982) 69.
[4] C.V. Barros Leite, E.F. da Silveira, J.M.F. Jeronymo, R.R. Pinho, G.B. Baptista, E.A. Schweikert, M.A. Park, Phys. Rev. B 45 (1992) 12218.
[5] R. Neugebauer, J.A.M. Pereira, R. Wünsch, T. Jalowy, K.O. Groeneveld, Nucl. Instr. and Meth. B 154 (1999) 325.
[6] J.A.M. Pereira, E.F. da Silveira, Phys. Rev. Lett. 84 (2000) 5904.
[7] G. Betz, K. Wien, Int. J. Mass Spectrom. Ion Process. 140 (1994) 1.
[8] J.A.M. Pereira, C.S.C. de Castro, J.M.F. Jeronymo, C.R. Ponciano, E.F. da Silveira, K. Wien, Nucl. Instr. and Meth. B 129 (1997) 21.
[9] M. Most, K. Wien, A. Brunelle, S. Della Negra, J. Depauw, D. Jaquet, M. Pautrat, Y. LeBeyec, Nucl. Instr. and Meth. B 164 (2000) 772, 168 (2000) 203.
[10] V. Mergel, R. Dörner, J. Ullrich, O. Jagutzki, S. Lencinas, S. Nüttgens, L. Spielberger, M. Unverzagt, C.L. Cocke, R.E. Olson, M. Schulz, U. Buck, E. Zanger, W. Theisinger, M. Isser, S. Geiss, H. Schmidt-Böcking, Phys. Rev. Lett. 74 (1995) 2200.
[11] Th. Weber, Kh. Khayyat, R. Dörner, V. Mergel, O. Jagutzki, L. Schmidt, F. Afaneh, A. Gonzales, C.L. Cocke, A.L. Anders, H. Schmidt-Böcking, J. Phys. B: Atom., Mol. Opt. Phys. 33 (2000) 3331.
[12] Th. Weber, H. Giessen, M. Weckenbrock, G. Urbasch, A. Staudte, L. Spielberger, O. Jagutzki, V. Mergel, F. Afaneh, M. Vollmer, R. Dörner, Nature 405 (2000) 658.
[13] CoboldPC (Computer Based Online Offline Listmode Dataanalyser), Roentdek, D-65779 Kelkheim, Germany.
[14] O. Jagutzki, V. Mergel, K. Ullmann-Pfleger, L. Spielberger, U. Meyer, R. Dörner, H. Schmidt-Böcking, in: M.R. Descour, S.S. Shen (Eds.), Imaging Spectrometry IV, Proceedings of SPIE, Vol. 3438, 1998, p. 322.
[15] O. Jagutzki, V. Mergel, K. Ullmann-Pfleger, L. Spielberger, U. Spillmann, R. Dörner, H. Schmidt-Böcking, Nucl. Instr. and Meth. A 477 (2002) 244.
[16] T. Jalowy, R. Neugebauer, M. Hattass, Th. Weber, R. Dörner, C.R. Ponciano, L.S. Farenzena, H. Schmidt-Böcking, E.F. da Silveira, K.O. Groeneveld, in preparation.